

SAN098-1357C
SAND-98-1357C
CONF-980731--

Optical Assembly of a Visible through Thermal Infrared Multispectral Imaging System

Tammy Henson
Sandia National Laboratories, P.O Box 5800, Albuquerque, NM 87185-0980

RECEIVED

Steve Bender and Don Byrd
Los Alamos National Laboratories, NIS Division, MS C323, Los Alamos, NM 87545

JUN 30 1998

William Rappoport and Gon-Yen Shen
Raytheon Optical Systems, Inc., 100 Wooster Heights Road, Danbury, CT 06810-7589

OSTI

Abstract

The Optical Assembly (OA) for the Multispectral Thermal Imager (MTI) program has been fabricated, assembled, and successfully tested for its performance. It represents a major milestone achieved towards completion of this earth observing E-O imaging sensor that is to be operated in low earth orbit. Along with its wide-field-of-view (WFOV), 1.82° along-track and 1.38° cross-track, and comprehensive on-board calibration system, the pushbroom imaging sensor employs a single mechanically cooled focal plane with 15 spectral bands covering a wavelength range from 0.45 to 10.7 μ m. The OA has an off-axis three-mirror anastigmatic (TMA) telescope with a 36-cm unobscured clear aperture. The two key performance criteria, 80% enpixeded energy in the visible and radiometric stability of 1% 1σ in the visible/near-infrared (VNIR) and short wavelength infrared (SWIR), of 1.45% 1σ in the medium wavelength infrared (MWIR), and of 0.53% 1σ long wavelength infrared (LWIR), as well as its low weight (less than 49 kg) and volume constraint (89 cm \times 44 cm \times 127 cm) drive the overall design configuration of the OA and fabrication requirements.

Keywords: Multispectral, Optical, Calibration, Telescope, Mirror, Space, Earth, Observing, Imaging, WFOV

Introduction

This paper describes the requirements, fabrication, assembly, and testing of the MTI OA that is part of the multispectral imaging system. The first section is a general description of the multispectral imaging system. The next several sections describe the OA performance requirements, OA system description, fabrication, integration and alignment, and testing. The last section is a summary.

Multispectral Imaging System General Description

The three major subsystems that make up the multispectral imaging system are the OA, the focal plane assembly (FPA), and the cryocooler. The OA has a 36 cm unobscured aperture and a 1.82° along-track and 1.38° cross-track WFOV. The OA provides high quality images from the visible through the thermal IR and also provides an accessible exit pupil in which to place a cold stop. The OA also consists of a state-of-the-art on-board calibration system (OBSCS). The OBSCS provides extremely stable sources to obtain accurate calibration on-board of the entire end-to-end imaging system and also of the FPA alone.

The FPA consists of linear detector arrays with optical filters immediately above the arrays. The detector arrays are placed at the focal plane of the OA. The linear arrays provide spatial resolution in one direction (cross-track). The motion of the pushbroom imaging system relative to the ground produces a scanning operation in the other direction (along-track), thereby producing two-dimensional images in multiple wavelength bands. The FPA also contains a cold shield, which extends from the detector arrays to the exit pupil of the OA. The FPA is enclosed in a vacuum shroud, with a BaF₂ window on the outside of the shroud which allows the light from the telescope to pass into the FPA. The window also allows the FPA to be evacuated separately and provides additional contamination control for the FPA. The thickness of each individual optical filter is adjusted so that the focal shift due to dispersion in the BaF₂ window and the optical filter substrates is equalized for all the bands and the focus is placed at the correct physical location for each detector array material type. A cold stop is placed at the exit pupil location. This design reduces the thermal background from the surrounding OA structure by allowing for 100% cold shielding.

DISCLAIMER

This report was prepared as an account of work sponsored by an agency of the United States Government. Neither the United States Government nor any agency thereof, nor any of their employees, makes any warranty, express or implied, or assumes any legal liability or responsibility for the accuracy, completeness, or usefulness of any information, apparatus, product, or process disclosed, or represents that its use would not infringe privately owned rights. Reference herein to any specific commercial product, process, or service by trade name, trademark, manufacturer, or otherwise does not necessarily constitute or imply its endorsement, recommendation, or favoring by the United States Government or any agency thereof. The views and opinions of authors expressed herein do not necessarily state or reflect those of the United States Government or any agency thereof.

DISCLAIMER

**Portions of this document may be illegible
in electronic image products. Images are
produced from the best available original
document.**

The linear arrays on the FPA are arranged in three pairs of sensor chip assemblies (SCAs). Each pair of SCAs consists of a visible wavelength to mid-wavelength infrared SCA and a long wavelength infrared SCA. The arrangement of the SCAs on the focal plane is shown in Figure 1. Three pairs of SCAs are used to span the full cross-track field of view. Bands A-D are the visible (VIS) bands whose spectral bandpasses are in the wavelength range of 0.45 - 0.86 microns. Bands E-G are near-infrared (NIR) bands whose spectral bandpasses are in the wavelength range of 0.86 - 1.04 microns. Bands H, I, and O are the short wavelength infrared (SWIR) bands whose spectral bandpasses are in the wavelength range of 1.36 - 2.35 microns. Bands J-K are medium wavelength infrared (MWIR) bands whose spectral bandpasses are in the wavelength range of 3.50 - 5.07 microns. Bands L-N are long wavelength infrared (LWIR) bands whose spectral bandpasses are in the wavelength range of 8.00 - 10.7 microns. Silicon photodiodes are used for bands A-D. Indium antimonide is used for bands E-K and O. Mercury cadmium telluride is used for bands L-N. The FPA, which was built by Raytheon Santa Barbara Research Center, is described in further detail in an IEEE paper given by J. Rienstra and M. Ballard¹.

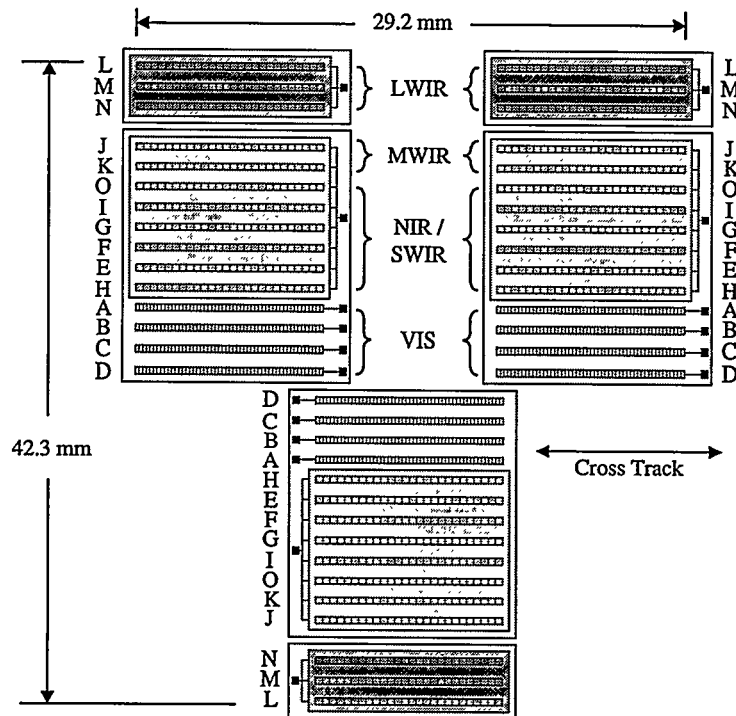


Figure 1. Focal plane layout.

A mechanical cryocooler is used to cool the FPA to a nominal temperature of 75 K. The cryocooler provides over 2.25 watts of cooling power at 65 K. A thermal strap connects the cold block of the cryocooler to a metal pedestal that supports the focal plane. A conservative 10 K increase in temperature across the thermal strap is assumed. The cryocooler also cools the cold shield to reduce the infrared background on the focal plane. The cryocooler uses temperature sensors to provide closed loop temperature control of the cold block. It is designed for low vibration to minimize jitter of the imaging system. The mechanical cryocooler was built by TRW.

Optical Assembly Performance Requirements

The OA performance requirements drove the OA design, fabrication and alignment tolerances, and testing criteria. The OA performance requirements are listed in Table 1. The need for a WFOV along with the physical size of the focal plane and the entrance aperture size dictated the need for a fast, F/3.47, optical system. The requirement for ensquared energy, flat focal surface, accessible exit pupil, and WFOV drove the design choice to an off-axis TMA

Requirement	Value
Entrance Aperture	36 cm diameter nominal
Paraxial Focal Length	125 cm nominal
Focal Plane Configuration	30.7 mm cross-track 43.2 mm along-track Band configuration shown in Figure 1
Focal Surface	Flat in the cross-track and along-track directions
Operating Wavelength	0.45 - 10.7 microns
Image Quality	(Measured at the detector surface. Includes BaF ₂ window and filter substrates.)
VIS	80% ensquared energy in 12.5 X 12.5 micron area
NIR, SWIR, & MWIR	84% ensquared energy in 50 X 50 micron area
LWIR	84% ensquared energy in 100 X 100 micron area
Effective Aperture Area	(Includes losses from BaF ₂ window but does not include losses through the detector spectral filters.)
VIS, NIR	825 cm ² (850 cm ² in band A)
SWIR, MWIR, & LWIR	860 cm ² (805 cm ² in band N)
Exit Pupil	Real accessible exit pupil at which a cold stop can be placed.
Stray Light	$\leq 10^{-6}$ for a point source at any angle ≥ 46 degrees off-axis
PST (out of field rejection)	
Veiling Glare (in field scatter)	For a uniformly illuminated field, $> 6\%$ of a pixel illumination shall be from light outside a radius given below for that pixels operating wavelength measured from the center of the pixel.
VIS	56.25 microns
NIR, SWIR, & MWIR	225 microns
LWIR	450 microns
Calibration Source Stability	Relative to the LANL Ground Calibration with NIST Traceability
VNIR/SWIR	1% 1 σ
MWIR	1.11% - 1.45% 1 σ
LWIR	0.53% - 0.68% 1 σ
Survival Temperature Range	-50 °C to +35 °C
Vibration and Shock	Meet all performance criteria after being subjected to vibration and shock levels consistent with a Taurus Launch Vehicle.
Volume	≤ 89 cm x 44 cm x127 cm
Weight	≤ 49 Kg

Table 1. Optical Assembly Performance Requirements

Design². The calibration requirements drove the design of the OBCS and the thermal control system. The optical design together with the OBCS design, weight, volume, and vibration requirements drove the mechanical design of the OA. The ensquared energy requirement, particularly in Band D, drove the fabrication and alignment tolerances of the system. The ensquared energy requirement must be met in any given band for all 3 SCAs simultaneously.

Optical Assembly System Description

Figure 2 shows the fully assembled OA in a Class 100 clean area at Raytheon Optical Systems, Inc, (ROSI). Figure 3 shows the OA integrated into the flight payload structure in the Class 100 clean area at Sandia National Laboratories (SNL). Once payload level assembly and testing is completed at SNL, the OA in the payload will be sent to Los Alamos National Laboratories (LANL) for ground calibration. Figure 4 illustrates the configuration of the OA system. The optical design is an off-axis TMA telescope. The primary and tertiary mirrors are tenth-order generalized aspheres, while the secondary mirror is a simple hyperbolic conic section. The three mirrors share a

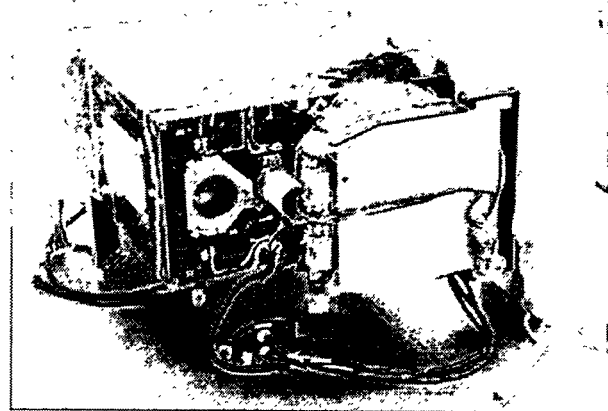


Figure 2. The fully assembled MTI Optical Assembly.

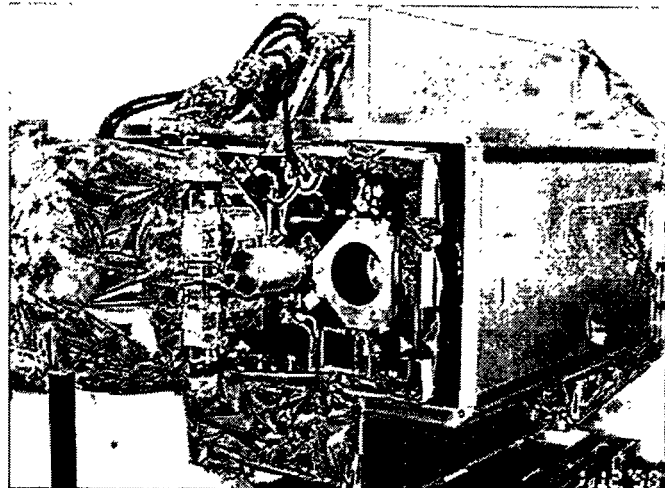


Figure 3. The MTI Optical Assembly in the Flight Payload Structure.

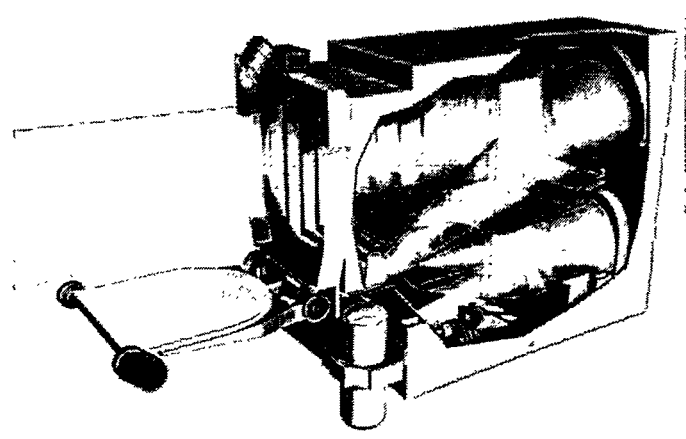


Figure 4. MTI Optical Assembly Configuration.

common optical axis, significantly reducing the complexity during alignment. The optical axis intersects the tertiary mirror near its center further aiding the alignment process. The mirrors are made of Zerodur. Both the primary and tertiary mirrors are aggressively lightweighted by 80% (Figure 5). The secondary mirror is mounted to an articulated mechanism capable of $\pm 150\text{-}\mu\text{m}$ focus adjustment at the focal plane.

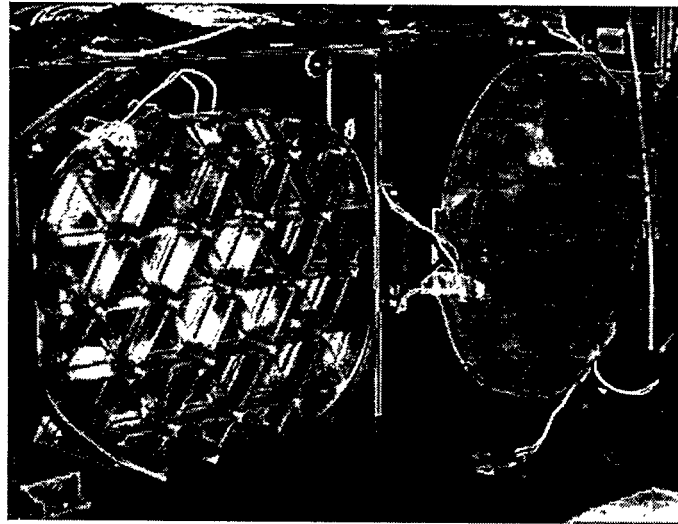


Figure 5. Primary and Tertiary Mirrors mounted on the OA Structure.

The main telescope structure is made of graphite cyanate ester composite material. This material provides extremely low thermal expansion and significantly lower dimensional changes due to water compared to graphite epoxy. The structure was fabricated by Alliant Techsystems, Inc., a Salt Lake City composite structure supplier. The temperature of the structure is actively controlled and continuously monitored with thermal sensors and heaters to maintain a stable background environment of the telescope.

Many of the complex mechanisms of the system stemmed from the need to provide both full aperture, end-to-end and "quick-look" calibrators, covering both visible and infrared wavelengths.

The full aperture calibrators are incorporated into the telescope's unique aperture door subassembly. The door is a double-clamshell design consisting of two motor extended panels, as depicted in Figure 6. The inside of the clamshell is painted white (Z-93P) for solar radiation diffusion. This panel, referred to as the Visible Reflectance Panel (VRP), can be folded or fully extended 180 degrees by a clutch/step motor driver. The top outside of the clamshell is painted black (Chemglaz Z306) as a blackbody source. The blackbody source is presented to the OA when the door is closed and the VRP is in the folded position. The bottom outside of the clamshell faces toward the scene when the door is closed. The door can be fully closed or open to 140 degrees during observation by two sets of clutch/motor drivers, one for primary use and one for redundancy.

For infrared band calibration, the blackbody is presented to the OA. The surface of the blackbody is precisely temperature controlled with heaters and thermistors to the pre-designated calibration temperature. During the visible calibration, the door is partially opened to 45 degrees and the VRP unfolded, exposing a white, diffused surface to receive the solar radiation at approximately a 47.5-degree compounded angle. The white surface diffusion characteristics are periodically calibrated with the Visible Reflectance Panel Monitor (VRPM) mounted on the door frame, which compares the irradiance of the solar illuminated panel to direct irradiance from the sun in five spectral bands.

During launch, the door is secured by a locking mechanism and will be released after the spacecraft reaches its operating orbit. During operations in space, the door is nominally closed to minimize heat leaks, and opened only during observation. In case of motor failure, the clutch can be de-energized and the door will spring open, as an extra safety measure. Similarly, the VRP goes to a closed position in the fail-safe mode.

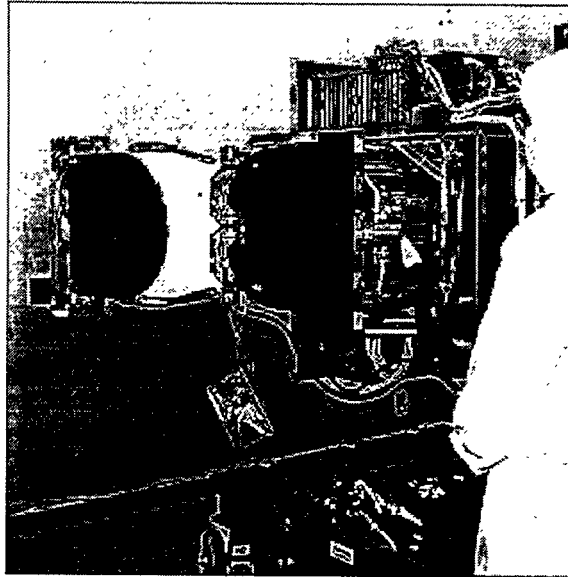


Figure 6. Baffle and Double-Clamshell Aperture Door

The quick-look calibrators are used for immediate reference before and after the scene imaging at both visible and infrared bands. The design has a five-position calibration wheel subassembly (Figure 7) located in front of the cold stop window of the focal plane dewar. The first position on the wheel, the nominal position, is an open position for viewing the far field. In the next position, a retro-reflection mirror is used to reflect the cryogenically cooled dewar view back into the focal plane thereby providing a near zero reference for the focal plane detectors. Thermistors on this mirror allow corrections for the actual temperature. The next two positions contain identical blackbody sources for thermal infrared calibration. These sources include a germanium lens that images the blackbody onto the focal plane. The blackbodies are temperature controlled and commandable up to 380 degrees Kelvin. Nominally, the two blackbodies are maintained at different temperatures which bracket the expected scene temperature. The last wheel position is for VNIR and SWIR calibration. It contains a lens and fold mirror which image light from a lamp assembly located off the wheel onto the focal plane. (A second lamp is built-in for redundancy). Photodiodes, which sense the lamp's intensity, are used in a feedback loop to provide a stable radiometric output and color temperature correction.

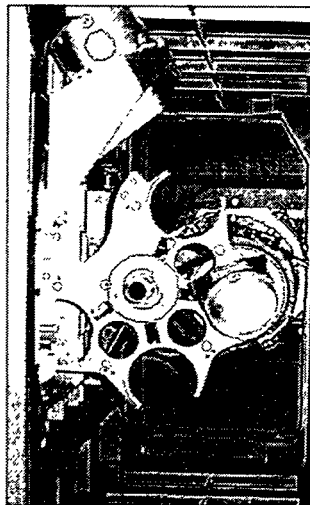


Figure 7. The quick-look calibration wheel subassembly provides immediate calibration before and after imaging.

The calibration wheel is a highly reliable mechanism driven by a set of clutch/step motor drivers (same design as the door subassembly, one primary and one for redundancy). The positioning of the various calibrators is very repeatable to minimize calibration errors at the focal plane. Again, the wheel has a clutch and a fail-safe spring that returns the wheel to its open position in case of motor failure.

The on-board radiometric calibration methodology that utilizes the various calibrator hardware at the various stages of the imaging operation is described in a paper by E. F. Zalewski³ and et. al. presented at the SPIE San Diego Conference 1998.

Fabrication

Fabrication of the OA consisted of three major tasks: optical fabrication, mechanical fabrication, and electrical fabrication.

Optical Fabrication

Optical fabrication of the MTI mirrors began with the Zerodur mirror blanks being shaped and then rough ground to near net shape. Controlled grinding was used to minimize the subsurface damage. The mirror blanks were left oversized during the entire grinding and polishing process to minimize any edge effects. During the rough figuring process, the mirror figure was monitored using the WEGU profilometer.

During the fine polishing process on the secondary mirror, the mirror figure was monitored using a Hindle sphere as the metrology tool. A parent mirror of approximately eight inches in diameter was then polished to the required 1/40 wave (rms at 0.633 μ m), and two off-axis segments were cut from the parent to yield two secondary mirrors, one for flight and one for use as a spare.

The final figuring on the tertiary mirror was accomplished using a computer-controlled polishing (CCP) technique and a diffractive null lens, fabricated by Diffraction International, as the metrology tool. The diffractive null proved to be of high quality, versatile, and cost effective. Once the final mirror figure was reached (1/40 wave rms over the footprint of an instantaneous field-of-view), the off-axis mirror was cut to its final geometry. The tertiary mirror then underwent lightweighting.

The primary mirror was figured and polished as an off-axis segment due to its large parent diameter (in excess of 1.2 meters). In addition to the fact that the primary mirror is very fast (f/0.6), polishing of the mirror was especially challenging because its vertex is not present within the mirror segment. In the transition from the coarse figuring to the fine polishing, two diffractive null designs were used. The center-of-curvature null has a larger dynamic range but coarser resolution, while the autocollimation-null provides the fine resolution sufficient for the final polishing and metrology. Again, the CCP technique was used for the primary mirror polishing operation prior to the shaping and lightweighting. The final figure achieved on the primary mirror was 1/21 waves rms during the final mirror metrology.

The lightweighting process involved removing material from the lightweight pockets, beveling, final shaping of the mounting features, and chemical etching to remove the damaged subsurface generated during the machining process. This polishing first, shaping/lightweighting afterward approach has been proven successful and highly beneficial. First of all, it was demonstrated that with proper operation, the mirror retained its pre-lightweight figure of 1/40 wave for the tertiary mirror and 1/21 wave for the primary mirror. Also, by polishing an oversized monolithic mirror first, we avoided any possibility of edge and quilting effects that could greatly complicate the operation if the mirror was shaped and lightweighted prior to polishing.

The coating on the mirrors is Denton FSS-99 protected silver (the specified coating for the multispectral sensor).

Details of the optical fabrication and metrology are described in an earlier paper⁴ presented at the SPIE Orlando Conference in 1998.

Mechanical Fabrication

The mechanical fabrication effort was focused on the three following key subassemblies, in addition to the graphite composite structure: the secondary mirror focusing mechanism, the aperture door subassembly, and the calibration wheel subassembly. The secondary mirror focusing mechanism was adapted from the High Altitude Balloon Experiment (HABE) secondary mirror mechanism design. To maintain dimensional stability, some of the aluminum mechanical elements were replaced with low thermal expansion invar. The aperture door mechanism driver and the wheel mechanism driver used identical designs; each adjusts torque transmission by changing the harmonic drive reduction ratio based on the required speed and reflective inertia for the specific drive trains.

The OA structure was fabricated using graphite cyanate ester with pseudo-isotropic fiber lay-up. The material has an order of magnitude lower moisture absorption property when compared with the older generation graphite epoxy composite. The coefficient of thermal expansion (CTE) along the fiber plane was slightly negative by design to counter the positive CTE of the titanium fittings. Thus, the end-to-end structural CTE is kept to a minimum, below 50 ppb/ $^{\circ}$ C. The various parts of the graphite structure were fabricated with sample coupon test to verify its design strength and stiffness. The structure was then assembled and underwent static load strength test in the process. The fully integrated structure was finally subjected to a full set of random vibration tests with mass simulators in place for the optics, baffle/door, calibrators, and FPA.

Electrical Fabrication

To control the thermal control elements of the telescope and drive the various mechanisms, four PC boards were designed, fabricated, and integrated into the Telescope Calibration and Control Electronics (TCAL) unit, a part of the overall sensor operation control electronics. The heaters, thermistors, and temperature controllers were attached to the telescope with wiring and cables providing connection to the TCAL.

Integration and Alignment

The most challenging task during the OA integration was the alignment and attachment of the three mirrors to the graphite structure. To accomplish the integration and alignment, three bipod flexures were first attached to the primary mirror and three to the tertiary mirror using CREST as the bonding agent. CREST was selected because its compliant nature at low temperature would prevent damage to the Zerodur mirror blanks. The secondary mirror was attached to three blade flexures on the focus mechanism also with a CREST bond.

These mirrors were then mounted to adjustable metrology mounts placed at proper relative locations to the telescope structure. Using a Zygo interferometer with a f/3.3 lens, the test beam was transmitted through the three mirrors and retro-reflected from a reference flat placed near the telescope entrance pupil that was oriented to the specific telescope field angle for testing in double-pass autocollimation configuration. Through an iterative process of adjusting the mirrors in all six degrees of freedom, the three mirrors converged to their designated positions. Since the telescope is a WFOV system, the final alignment was established using ROSI's Computer Aided Alignment Optimization (CAAO) technique to meet wavefront requirements at all field angles within the design FOV.

At this stage, the flexures on the primary and tertiary mirror as well as the mounting flange of the secondary mirror mechanism were attached to the graphite structure using EC2216 epoxy. After a 72-hour setting period for the epoxy, the adjustable metrology mounts were detached from the mirrors and mirror mechanism, thus completing the OA alignment.

The aperture door and the calibration wheel subassemblies were then mounted to the structure through a set of flexures completing the telescope integration.

Testing

The system testing program for the OA consisted of 14 categories, including the full field wavefront test, the calibrator performance test, the thermal vacuum test, and random vibration and shock test. The OA successfully passed all tests.

Full-Field Wavefront Test

The MTI OA is a WFOV system. In meeting the image quality requirement, the wavefront performance was validated through interferometric testing over the full field of view. This test was accomplished with a double-pass autocollimation arrangement using a surrogate focal plane fixture for defining the system exit pupil and focal locations. The surrogate focal plane consists of a BaF₂ window, a pupil stop, an SF11 surrogate filter substrate (identical to the FPA arrangement for Band D), and a set of 11 discrete spherical balls distributed at the extremes and center of the FPA FOV.

During testing, the interferometric test beam was first focused onto one of the balls corresponding to the field angle to be tested. The balls were subsequently removed and the beam was propagated through the OA and autocollimated back from the retro-flat, located near the telescope entrance, which was adjusted to return the collimated output back to the interferometer in a double-pass configuration. The measured wavefront at the interferometer was recorded. The wavefront, as measured at several points across the field, met the requirement at all points.

Post-processing of the test data established that the flatness of the focal plane locations is well within the measurement accuracy of less than 3 μm . Also, the image distortion characteristics of the as-built OA was measured, and corresponded to the design prediction well within 1%.

To access the effect of the gravity on the telescope wavefront performance, the OA wavefront was measured after it was rotated 180 degrees. The overall 1-g effect is 0.065 waves rms, a small portion of the overall wavefront budget and meeting the requirement.

The wavefront of the OA was later tested after the random vibration/shock test, and essentially the same results were obtained. The wavefront test demonstrated that the MTI OA met the imaging quality requirement of 80% enpixeded energy in the visible bands (12.5- μm pixels) and 84% enpixeded energy in the infrared bands (50- μm pixels, 84% in 100 μm square in the LWIR).

Utilizing the as-built OA prescription, the wavefront data taken across the FOV, and the as-built FPA parameters, the MTF was determined at the Nyquist frequency for all 15 spectral bands at several field locations and then compared with the diffraction MTF at those field locations. The Nyquist frequency is determined by the size of the pixel used to sample the image. For the visible bands A - D the Nyquist frequency is 40 cycles/mm, and for the infrared bands E - O the Nyquist frequency is 10 cycles/mm. Figure 8 shows the average MTF at Nyquist frequency of the as-built OA/FPA across the FOV for each spectral band of the system. The average diffraction-limited MTF at Nyquist frequency across the FOV for each spectral band is also shown for comparison. It is clear to see that the performance of the as-built OA/FPA is diffraction-limited beyond about 0.9 μm wavelength at the Nyquist frequency.

Calibration Performance Test

The calibration hardware underwent extensive testing to assure it would meet the radiometric stability requirements. All radiometric stability requirements are relative to the LANL ground calibration that will be performed with NIST traceability.

A particular concern was that the quick calibration visible source would repeat within budgeted allocations after vibration. This verification was performed at the calibration wheel subassembly level. The test included effects both due to vibration and repeatability of repositioning the wheel. The irradiance values repeat within the budgeted \pm 0.7% across the required 42-mm field.

Although the VRPM is used only for relative measurements, it needed an absolute calibration to ensure that its outputs would be within the range of the data acquisition system. This was done in two parts. First, the system was calibrated against the ROSI Precision Radiometric Source (PRS), which has calibration traceable to England's National Physical Laboratories. This gave the relative calibration in each band, but did not fill the VRPM FOV. Secondly, the unit was tested outdoors at SNL under clear skies with a surrogate diffuse panel. The comparison of the two data sets allowed for correction in the outdoor data for atmospheric absorption. The VRPM spectral and field-of-view response characterization was performed at SNL as well.

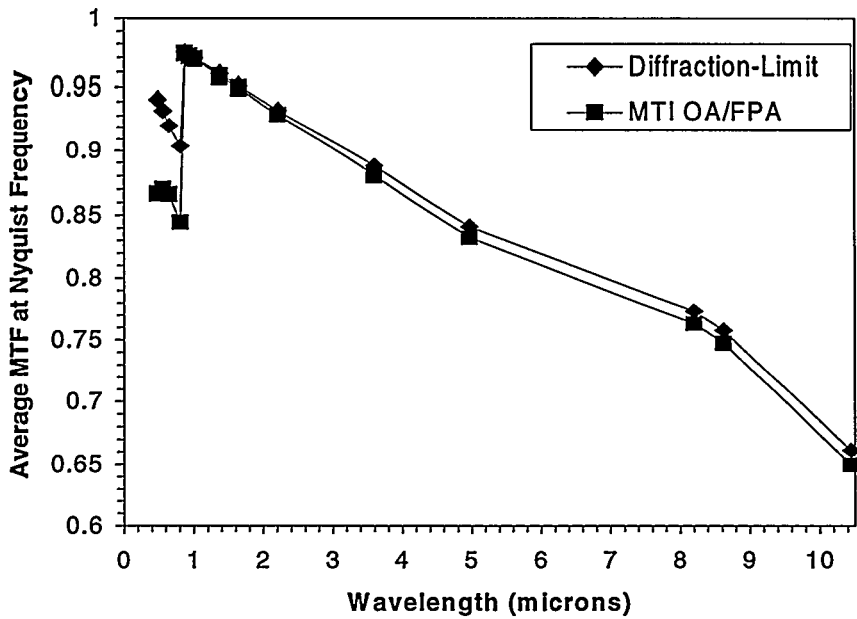


Figure 8. Average MTF at Nyquist frequency compared to the diffraction-limit across the FOV for each spectral band.

The IR calibration source performance depends on stable thermistors. We learned that the mounting technique was critical to thermistor measurement stability. The RTV's used to mount the thermistors were sufficiently hard at -50°C to change the calibration of the thermistor permanently. When we searched for an RTV that would remain soft at temperatures well below -50°C we found GE RTV-566 which was used by the Moderate Resolution Imaging Spectroradiometer (MODIS) program in mounting their platinum resistance thermometers. The GE RTV-566 remains soft at temperatures as low as -115°C . Mounting the thermistors with GE RTV 566, SNL confirmed the stability of the thermistors to 50 mK in their mounted configuration under temperature cycling from -50°C to $+110^{\circ}\text{C}$ and vibration by measuring the resistance of the thermistors in a well controlled ice bath at every stage of fabrication and testing.

The OBCS quick-look blackbodies were qualified as a subassembly for radiometric stability, uniformity and output flux. Stability and uniformity characterization of the OBCS output was accomplished with the use of a single element, liquid nitrogen cooled HgCdTe detector whose output was filtered with a lock-in amplifier. Flux levels were referenced to a four inch aperture water bath blackbody source that was built and calibrated by NIST. The test set-up duplicated the geometry of a single pixel in the focal plane viewing the blackbodies through the Lyot stop. Examination of arbitrary pixel locations was supported by placement of the detector on the center of rotation of a dual gimbal arrangement which was mounted on two orthogonal translation stages.

Short term stability of the detector and OBCS quick-look blackbodies combined showed a max variation of 0.04% over a two hour period with an RMS measurement precision of approximately 0.006%. For reference, orbital calibration and image collection sequences are on time scales of less than 10 minutes. Long term stability measurements were limited by replication of the test set-up geometries, the detector itself referenced to the NIST blackbody produced a maximum variation of $\pm 2.8\%$ over several months. Observed repeatability of the OBCS blackbodies over a five month period was within this measurement uncertainty and was 2.1% for SN1 and 1.0% for SN2.

Uniformity of the quick-look blackbody output in the focal plane was obtained by raster scanning the detector element using the translation stages and repointing to the Lyot stop using the two gimbaled axes. The gimbal pointing increased the incident flux on the detector compared to a flat focal plane and the output values were subsequently "cosine" corrected. Both blackbodies showed nearly identical uniformity with values of approximately

0.17%/mm and 0.2%/mm being measured for the along track and cross track directions, respectively. The specified irradiance uniformity in the focal plane was 0.2%/mm.

Output of the two quick-look blackbodies differed from one another by approximately 11% when they were controlled to the same temperature. At the present time the source of this difference is not known but it appears to be stable and does not present a problem. No independent radiometric calibration of the OBGS blackbodies was required at the subassembly level since their calibration will be established at the system level. Their nominal performance was compared to the NIST water bath blackbody and they were found to produce an equivalent detector output at NIST blackbody temperatures approximately 22 degrees cooler than their own control temperatures.

The results of the calibration source tests were all within the amounts budgeted to assure the radiometric stability requirements would be met.

Thermal Vacuum Test

The MTI OA, which will be operated in space at a nominal temperature of 275 degrees Kelvin, is designed to survive a high temperature of 308 degrees Kelvin and a low of 223 degrees Kelvin. The objectives of the thermal vacuum test were: (1) verify the operation of the thermal control components; (2) verify that the wavefront performance meets the imaging quality requirement at the nominal operating temperature in a vacuum environment; (3) verify the operation of all mechanisms and calibration sources in vacuum; and (4) subject the OA to the survival temperature extremes.

To meet the first objective, the OA was installed in the vacuum environment and cooled to below the 275 K operating temperature. The thermal control system was then enabled, and the OA warmed to the control setpoint. The optical wavefront was measured in a double-pass configuration using a Zygo interferometer located outside the vacuum chamber, along with a 16-inch collimating lens inside; the test beam was retro-reflected from spherical balls located on a surrogate focal plane test fixture.

During the cool down, all thermal control elements were functioning properly and the temperature profile was very close to the analytical prediction. All mechanisms and calibration sources were exercised at the operating temperature.

The wavefront test result indicated that the change in pressure and temperature only slightly altered the OA wavefront performance by approximately 0.05 waves rms. Afterward, the OA was brought to the extreme temperatures. The post survival temperature test indicated that the OA survived the test with all its functions working properly and essentially maintaining its wavefront performance.

Random Vibration and Shock Test. After the thermal vacuum test, the OA was random vibration and shock tested to validate its structural integrity during satellite launch. Post vibration/shock optical performance and functional test verified that the optical performance met end-to-end system requirements.

Summary

In summary, we have successfully completed the OA assembly and test with performance meeting or exceeding the specification. This state-of-the-art telescope with its on-board calibration system is currently being integrated with the other payload components prior to the ground calibration and integration into the satellite.

References

1. J. Rienstra and M. Ballard, "Multispectral Focal Plane Assembly for Satellite Remote Sensing", 1998 IEEE Aerospace Conference Proceedings, March 21-28, 1998, 7.502.
2. K. Shu, and T. Henson, "Optical design for a Visible through Thermal Infrared Multi-Band Imaging System", SPIE Proc. Vol. 2863, p. 301 (1996).

3. E. Zalewski, W. Rappoport, F. Sileo, J. Stein, G. Huse, S. Bender, and P. Thacher, "On-board Calibration System for a Visible to Thermal Multispectral Imaging Sensor", SPIE Proc. Vol. 3439, (1998).
4. J. Magner, and T. Henson, "Optical fabrication and metrology for a Visible through Thermal Infrared Multi-Band Imaging System", SPIE Proc. Vol. 3377, (1998).

Sandia is a multiprogram laboratory operated by Sandia Corporation, a Lockheed Martin Company, for the United States Department of Energy under Contract DE-AC04-94-AL85000.